Analysis and Simulation of 3D Trajectory with Obstacle Avoidance of an Autonomous Underwater Vehicle for Optimum Performance

Sami A, Mostafa[*]   and   **Ayman M. M. Brisha****

Suez Canal University, Faculty of Industrial Education,   Beni Suef University, Faculty of Industrial Education,
Egypt   Egypt

Summary

The navigation of an autonomous underwater vehicle in both horizontal and vertical planes is considered a problem that has to be solved. Obstacle avoidance for such vehicles while path following in X_Z plane is also considered a point under research. In the present work, a proposed obstacle avoidance while path following (OAWPF) algorithm is designed to simulate the 3D trajectory of such a vehicle. Different obstacle shapes are used to evaluate the algorithm performance in both horizontal and vertical planes. The dynamics of the vehicle and the sea floor environmental conditions are analyzed while designing the OAWPF algorithm. A Matlab programming environment is utilized to simulate and evaluate the algorithm. The results show that the algorithm is robust and dynamic. It improves and secures the vehicle navigation against facing obstacles.

Key words:

AUV Path planning, AUV 3D trajectory, Obstacle avoidance, OAWPF algorithm.

1. Introduction

Over the last few years, autonomous underwater vehicles (AUVs) have been frequently used for fishery studies, sea bottom exploration, mine-searching, scientific and oceanic data gathering, reconnaissance, and many other purposes [1]. The design of AUVs still needs development in order for them to completely carry out missions in spite of the obstacles they may face. Different types of AUVs have been designed and built to undertake such missions, such as VideoRay Pro III micro, the Experimental Fluids Lab, the University of Waterloo, that of the U.S. Navy together with the Environmental Protection Agency, the Autonomous Undersea Systems Institute Solar Powered Autonomous Underwater Vehicle (SAUV II), the Maya AUV developed at the National Institute of Oceanography (NIO, Goa, India), the U.S. Naval Postgraduate School REMUS, and the NPS ARIES [2].

In this paper, the REMUS will be used as an example of the AUV model. The design features and characteristics of the REMUS AUV were defined and its performance was tested in [3]-[4]. This work utilizes the features and dynamics of this vehicle to test and evaluate the proposed

OAWPF algorithm. Note that this algorithm can be applied to any AUV with some modifications concerning the vehicle data and characteristics.

2. Remus Auv

The Remote Environmental Monitoring Units (REMUS) vehicle was developed at Wood's Hole Oceanographic Institute (WHOI) in the Oceanographic Systems Laboratory. It is designed to perform hydrographical reconnaissance in the very shallow water (VSW) zone from 40 to 100 feet (Fig. 1).

Fig. 1. REMUS AUV.

It has low cost and is lightweight. The vehicle operates with a laptop computer and simplifies launching and recovery operations due to its compact size and light weight. REMUS is considered an attractive platform for AUV study and research. All REMUS data and detailed characteristics of physical features and functional capabilities are taken from [3]-[4].

3. Problem Definition and Previous work

The problem under investigation concerns mainly the design of the AUV trajectory in a dynamic environment where it is supposed that the vehicle may face obstacles of different types. The vehicle's motion is discussed in the horizontal and vertical planes. The effectiveness of the AUV designed trajectory is based upon the probability that it can successfully overcome obstacles and complete its mission. Thus, an obstacle avoidance while path following (OAWPF) algorithm is proposed to work in conjunction

with the planned path follower, the auto pilot, to secure navigation of the vehicle and increase the vehicle's ability to avoid unknown obstacles. During the last two decades, much effort has been put into exploring subjects concerning the development of AUV path planning and obstacle avoidance. A dynamic model of an AUV presented in [5] has been carried out for optimum path planning to perform certain missions, but no obstacles have been assumed. A horizontal path planning algorithm for the REMUS AUV with obstacle avoidance is designed in [6]-[7]. The results are considered satisfactory, but the motion is discussed only in the horizontal plane. A depth control of AUV motion studied in [8] for the INFANTE AUV, built and operated by the Instituto Superior Te ´ cnico of Lisbon, Portugal, achieved good results in controlling vehicle depth, disregarding the motion in the X_Y plane. The same study carried out considering only the motion in the vertical plane was done by Pramod et al. [10]. The MAYA AUV horizontal and vertical motion was discussed in [10], but without considering obstacles. Thus, analysing and evaluating the 3D motion of an AUV is considered a problem that has to be addressed.

4. Vehicle Equations of Motion

The equations of motion that describe the vehicle navigation control have to be stated accurately to achieve acceptable simulation results. Assume that the vehicle is moving as a rigid body without any influence of the earth's rotation upon its centre of mass, and the main acting forces are either inertial or gravitational forces. Hydrostatic, hydrodynamic forces resulting from lift and drag components, and propulsion thrusting force are the main forces acting upon the vehicle body. In general, the rotational and translational equations of motion for the six degree of freedom model shown in Fig. 2 are written as follows [11]:

$$\eta_1 = \begin{bmatrix} x & y & z \end{bmatrix}^T; \qquad \eta_2 = \begin{bmatrix} \phi & \theta & \psi \end{bmatrix}^T$$
$$v_1 = \begin{bmatrix} u & v & w \end{bmatrix}^T; \qquad v_2 = \begin{bmatrix} p & q & r \end{bmatrix}^T$$
$$\tau_1 = \begin{bmatrix} X & Y & Z \end{bmatrix}^T; \qquad \tau_2 = \begin{bmatrix} K & M & N \end{bmatrix}^T$$
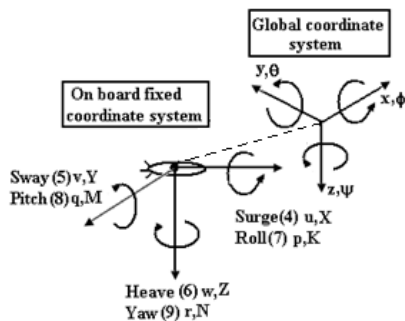

Fig. 2 Coordinate systems with angles transformation.

where η_1, η_2, describe the position and orientation of the vehicle fixed coordinate system with respect to the global fixed coordinate system; v_1, v_2, are the translational and rotational velocities of the vehicle fixed coordinate system with respect to the global fixed coordinate system; and τ_1, τ_2, are the total forces and moments acting on the vehicle with respect to the body-fixed reference frame. Note that the numbers that appear in Fig. 2 are the numbers of the corresponding equations, Eqs. 1 to 9, which describe the variables. Translational velocities between the vehicle and the global fixed coordinate systems are related as follows:

$$\begin{bmatrix} \dot{x} \\ \dot{y} \\ \dot{z} \end{bmatrix} = T * \begin{bmatrix} u \\ v \\ w \end{bmatrix} \qquad (1)$$

The transformation matrix T is defined in terms of the Euler angles (φ,θ,ψ) as follows:

$$T(\phi,\theta,\psi) = \begin{bmatrix} \cos\psi\cos\theta & \sin\psi\cos\theta & -\sin\theta \\ \cos\psi\sin\theta\sin\phi - \sin\psi\cos\phi & \sin\psi\sin\theta\sin\phi + \cos\psi\cos\phi & \cos\theta\sin\phi \\ \cos\psi\sin\theta\cos\phi + \sin\psi\sin\phi & \sin\psi\sin\theta\cos\phi - \cos\psi\sin\phi & \cos\theta\cos\phi \end{bmatrix} \quad (2)$$

The rotational velocities between the fixed and the global coordinate systems of the vehicle are related as follows:

$$\begin{bmatrix} p \\ q \\ r \end{bmatrix} = \begin{bmatrix} 1 & 0 & -\sin\theta \\ 0 & \cos\phi & \sin\phi\cos\theta \\ 0 & -\sin\psi & \cos\phi\cos\theta \end{bmatrix} \begin{bmatrix} \dot{\phi} \\ \dot{\theta} \\ \dot{\psi} \end{bmatrix} \qquad (3)$$

Note that for small angles: $p = \dot{\phi}, \quad q = \dot{\theta}, \quad r = \dot{\psi}$.

The local velocity is a vector composed of three components: surge (u), sway (v), and heave (w). The equations of motions considering these components are written as follows [7]:

- Surge, translation about x axis, equation of motion:

$$m[\dot{u}_r - v_r r + w_r q - x_G(q^2 + r^2) + y_G(pq - \dot{r}) +$$
$$z_G(pr + \dot{q})] + (W - B)\sin\theta = X \qquad (4)$$

- Sway, translation along y axis equation of motion:

$$m[\dot{v}_r + u_r r - w_r p + x_G(pq + \dot{r}) - y_G(p^2 + r^2) +$$
$$z_G(qr - \dot{p})] - (W - B)\cos\theta\sin\phi = Y \qquad (5)$$

- Heave, translation along z axis, equation of motion

$$m[\dot{w}_r - u_r q + v_r p + x_G(pr - \dot{q}) + y_G(qr + \dot{p}) -$$
$$z_G(p^2 + q^2)] - (W - B)\cos\theta\cos\phi = Z \qquad (6)$$

- Roll, rotation about x axis, equation of motion

$$I_x \dot{p} + (I_z - I_y)qr + I_{xy}(pr - \dot{q}) - I_{yz}(q^2 - r^2) - I_{xz}(pq$$
$$+ \dot{r}) + m[y_G(\dot{w}_r - u_r q + v_r p) - z_G(\dot{v}_r + u_r r - w_r p)] -$$
$$(y_G W - y_B B)\cos\theta\cos\phi + (z_G W - z_B B)\cos\theta\sin\phi = K \qquad (7)$$

- Pitch, rotation about y axis, equation of motion

$$I_y\,\dot{q}+(I_x-I_z)pr-I_{xy}(qr+\dot{p})+I_{yz}(pq-\dot{r})+I_{xz}(p^2$$

$$-r^2)-m[x_G(\dot{w}_r-u_rq+v_rp)-z_G(\dot{u}_r-v_rr-w_rq)]+$$

$$(x_GW-x_BB)\cos\theta\cos\phi+(z_GW-z_BB)\sin\theta=M \qquad (8)$$

- Yaw, rotation about z axis, equation of motion

$$I_z\,\dot{r}+(I_y-I_x)pq-I_{xy}(p^2-q^2)-I_{yz}(pr+\dot{q})+I_{xz}(qr$$

$$-\dot{p})+m[x_G(\dot{v}_r+u_rr-w_rp)-y_G(\dot{u}_r-v_rr+w_rq)]-$$

$$(x_GW-x_BB)\cos\theta\sin\phi-(y_GW-y_BB)\sin\theta=N \qquad (9)$$

where:

I_x, I_y, I_z ……. mass moment of inertia.

u_r, v_r, w_r …….velocity components of the vehicle fixed system w.r.t. water.

x_B, y_B, z_B ……distance between geometric centre and centre of buoyancy of the vehicle.

x_G, y_G, z_G ….. distance between the centre of gravity and the geometric centre of the vehicle.

B …………... Buoyancy, W …………... Weight.

X, Y, Z, K, M, N …. Sums of all external forces and moments acting on the vehicle rigid body.

Equation (10) represents the final equation of motion of the vehicle considering the hydrodynamic coefficients associated with REMUS to create the final equation used to model the motion of REMUS [12].

$$\begin{bmatrix} m-Y_{\dot{v}_r} & 0 & 0 \\ 0 & I_{zz}-N_{\dot{t}} & 0 \\ 0 & 0 & 1 \end{bmatrix}\begin{bmatrix} \dot{v}_r \\ \dot{r} \\ \dot{\psi} \end{bmatrix}=\begin{bmatrix} Y_{v_r} & Y_r-mU & 0 \\ N_{v_r} & N_r & 0 \\ 0 & 0 & 1 \end{bmatrix}\begin{bmatrix} v_r \\ r \\ \psi \end{bmatrix}+\begin{bmatrix} Y_\delta \\ N_\delta \\ 0 \end{bmatrix}\delta_r(t) \quad (10)$$

where $\delta_r(t)$ is the delta function of the rudder.

4.1 Vehicle Equations of Motion in the Horizontal Plane

Considering only the motion of the vehicle in the horizontal plane, the following assumptions can be made [6]:

- Motion in the vertical plane is negligible, which means that the values of w_r, p, q, r, Z, φ, and θ are all zero.

- The speed u_r is equal to the forward speed U_o, resulting in $\dot{\psi}=r$. Thus, the equations of motion are simplified as follows [6]-[7]:

$$m\,\dot{v}_r=-mU_or+\Delta Y(t) \qquad (11)$$

$$I_{zz}\dot{r}=\Delta N(t) \qquad (12)$$

$$\dot{X}=U_o\cos\psi\text{ - }v_r\sin\psi+U_{cx} \qquad (13)$$

$$\dot{Y}=U_o\sin\psi\text{ - }v_r\cos\psi+U_{cy} \qquad (14)$$

4.2 Vehicle Equations of Motion in the Vertical Plane

Considering only the vehicle motion in the vertical plane, the following assumptions can be made:

- p = 0, $\dot{p}$ = 0, $v=0$, $\dot{v}=0$, r = 0, $\dot{q}=0$

- Only z_G has a value while the values of x_G, y_G, x_B, y_B, and z_B are all zero. Thus, the equations of motion are simplified as follows [13]:

$$m\,\dot{w}_r-mU_oq-(W-B)=Z(t) \qquad (15)$$

$$I_y\,\dot{q}+z_G\,W\sin\theta=M(t) \qquad (16)$$

$$\dot{\theta}=q\cos\phi=q \qquad (17)$$

$$\dot{Z}=\text{-}U_o\sin\theta+w_r\cos\theta\cos\phi \qquad (18)$$

where U_o is the forward speed.

5. Navigation and Guidance Control

Most of the known navigation control algorithms implement waypoints following schemes assuming that the vehicle is given coordination of a sequence of waypoints *a priori* in the region of interest. These waypoints are connected to generate the overall planned vehicle mission path. Fig. 3 shows a proposed planned vehicle mission path consisting of six waypoints interconnected with five tracks.
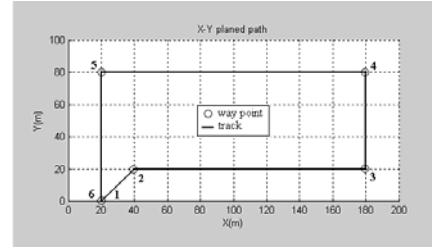

Fig. 3 X-Y vehicle path way-points and tracks.

The sliding mode control (SMC) is utilized for steering, speed, and depth control of the vehicle. In navigation applications, SMC has been shown to be quite satisfactory in controlling a slow AUV like REMUS. The equations of motion that describe the vehicle's horizontal and vertical motions, Eqs. 11 to 18, are treated separately as three linear, independent, and single-input single-output systems for speed, heading, and depth. Hereby, the SMC technique as an application will be introduced rather than the SMC theory. More details are presented in [14].

5.1 SMC for REMUS AUV

To create the SMC, the general form of the equations of motion is considered as:

$$\dot{x} = A\,x + Bu \qquad (19)$$

where $x \in R^{n*1}, A \in R^{n*n}, B \in R^{n*r}, u \in R^{r*1}$, and u is either the rudder angle for the vehicle horizontal motion controller, or the elevator angle for the vehicle vertical motion controller. A sliding surface σ is then created, in which $\sigma = 0, \sigma \in R^{\rho*1}$. The sliding surface is thus defined

as $\sigma = s'\,\tilde{x}, \tilde{x} = x - x_{com}$, where s' is a vector of directions in the state error space. As discussed in SMC theory [14], the controller works by driving the sliding surface to zero. As the sliding surface approaches zero, the error between the state variable (x) and the command (x_{com}) is zero. By definition of the sliding mode controller, the system dynamics must exhibit stable sliding on the surface when σ = 0. Therefore, s' can be determined by observing that the closed loop dynamics are given by the poles of the closed loop matrix as

$$(A - bk_2) = A_c, \text{ with } k_2 = [s'B]^{-1}s'A$$

where k_2 is chosen by pole placement and $A_c s' = 0$ to achieve the condition σ = 0. Getting the eigenvectors of the A_c matrix, the feedback gains for each state can be found. Thus, the sliding surface for the horizontal motion is as follows:

$$\sigma(t) = s_2 * (r_{com} - r(t)) + s_3 * \dot{\psi}_{LOS}(t) \qquad (20)$$

where LOS stands for line of sight. The commanded rudder, dr(t), in the LOS controller becomes:

$$dr(t) = -k_2 * r(t) * \eta * \tanh(\sigma(t)/\phi) \qquad (21)$$

The sliding surface for the vertical motion is as follows:

$$\sigma(t) = -s_1 q(t) - s_0 w_r(t) + s_2(\theta_{com} - \theta(t)) + s_3(Z_{com} - Z(t)) \quad (22)$$

and the commanded elevation angle δ(t) becomes:

$$\delta(t) = -k * x - \eta * \tanh(\sigma(t)/\varphi) \qquad (23)$$

where η and φ are tuning factors.
SMC is coupled with a LOS guidance scheme to describe a desired vehicle path that provides waypoints. Waypoints navigation based on LOS guidance is used to achieve path tracking.

5.2 LOS Guidance

LOS is the most widely used guidance method today. Most guidance methods used today have some form of LOS guidance because of its simplicity and ease of implementation. Simply, LOS guidance is used to maintain vehicle path tracking by looking ahead to prescribed waypoints. The LOS guidance employs the LOS angle between the vehicle recent position and the vehicle planned position. The LOS angle ψ_{LOS} can easily be calculated as follows:

$$\psi_{LOS} = \tan^{-1}\left(\frac{y_2 - y_1}{x_2 - x_1}\right) \qquad (24)$$

where (x_1, y_1) and (x_2, y_2) are the recent and future position coordinates, respectively. The LOS control system is illustrated in Fig. 4.
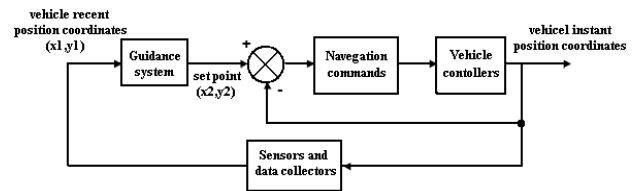

Fig. 4 LOS control system.

6. OAWPF Algorithm

While the vehicle is following the planned mission path, it is assumed that the autopilot maintains the vehicle's forward speed and depth, altitude from the sea bottom, constant. The obstacles that the vehicle may face while path following are detected using a model of a two-dimensional forward-looking sonar with a wide horizontal angle scan and a sufficiently long radial range. Fig. 5 illustrates the sonar scanning technique of an obstacle.
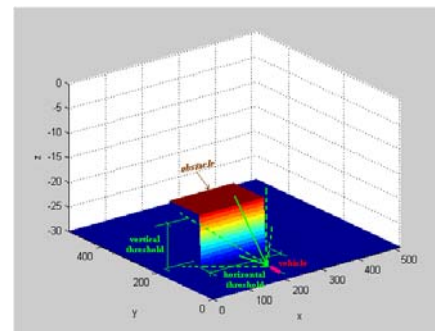

Fig. 5 Forward-looking sonar scanning an obstacle.

According to the forward-looking sonar specifications, the observed obstacle x, and z data collected are classified and calibrated with the maximum manoeuvring capabilities of

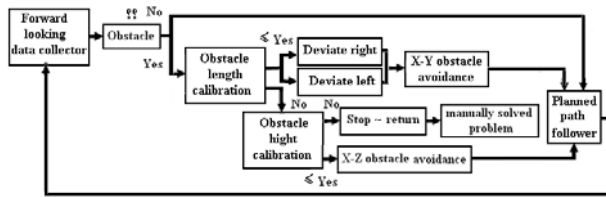the guidance controllers in both the horizontal and vertical planes. The OAWPF algorithm is modelled in Fig. 6.

Fig. 6 Steps of QAWPF algorithm.

During a prescribed mission, the vehicle automatically follows the waypoints tracks. If the vehicle accidentally faces an obstacle, additional factors will be added to the system dynamics to modify the vehicle trajectory for the sake of avoiding the obstacle. An additional heading angle, $\pm \psi_{ob}$, must be added to the calculated path following heading angle $\psi(t)$ when trying to avoid an obstacle in the $X-Y$ plane. The $\pm$ for the ψ_{ob} means deviating right or left. Another factor, which is an additional altitude, $\pm H_{add}$, must be added to the depth following the controller when trying to climb over a vertical obstacle. The sign + is used when climbing over the obstacle, while the sign – is used when descending, leaving the obstacle and following the initial path depth. The overall system dynamics with obstacle avoidance mechanism while path following are described in Fig. 7.
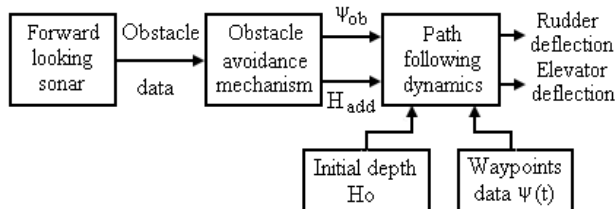
Fig. 7 System dynamics with obstacle avoidance.

7. Simulation Results, Analysis, and Evaluation

The Matlab programming environment is utilized to simulate and evaluate the proposed OAWPF algorithm. The REMUS vehicle characteristics data and dynamics are used while solving the equations of motion of the AUV vehicle. The used forward-looking sonar model has a horizontal range of about 30 m, and a beam vertical angle of about 25°. The vehicle must maintain an altitude of about 3m above the sea floor as a sufficient, safe distance.
The vehicle starts its mission following the suggested path track with the predetermined waypoints shown in Fig. 3. To evaluate the proposed OAWPF algorithm, a quite sufficient number, i.e., eight, of arbitrarily selected

obstacles with different x-y dimensions and different x-y locations are used along the vehicle path as shown in Fig. 8. Applying the OAWPF algorithm, the vehicle's dynamic x-y trajectory against those obstacles is drawn in Fig. 8. A 3D look at the vehicle trajectory is shown in Fig. 9. From Figs. 8 and 9 it can be seen that the proposed algorithm can correctly decide what direction is more easy to follow while avoiding the facing obstacles.
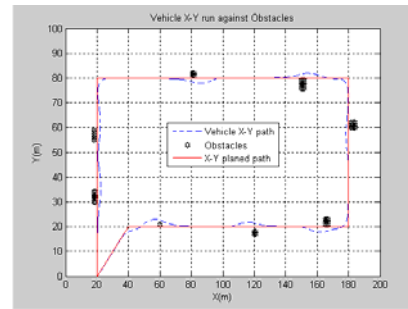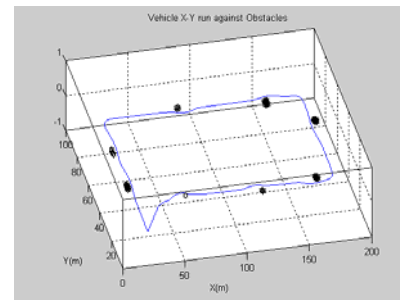

Fig. 8 Vehicle run against facing obstacles.

Fig. 9 3D look at the vehicle's x-y path against obstacles.

The outputs of the vehicle's dynamics controller, rudder deflection, heading angle, and the added heading angles necessary for avoiding each obstacle are shown in Fig. 10.
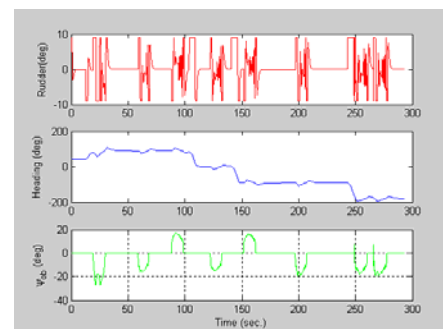

Fig. 10 Vehicle controller outputs in the X-Y plane.

It can be seen from Fig. 10 that the rudder deflection is approximately symmetric around the zero angle, which means that the vehicle is going forward along the planned

path and the rudder is being deflected right or left to avoid the obstacle and then left or right to go back to the planned path. The heading angle starts with an initial value to go directly to the planned track. The heading angle keeps positive values while avoiding the first three obstacles, i.e., during the first part of the planned path. Then the heading values increase in the negative direction to go left three times to complete the mission. The value and time duration of each added ψ_{ob} angle is shown in the third row in Fig. 10. The shown ψ_{ob} data describe which side and how long the vehicle takes to avoid the obstacle.

For example, the vehicle needed more time and more negative ψ_{ob} to avoid the first obstacle. At the time the heading angle of the vehicle is changing to follow the second track, the vehicle faces the first obstacle. The vehicle goes left to avoid the obstacle while going right to follow the waypoints track. Thus, the value of ψ_{ob} is more, and the time is more and the sign is negative. The same procedure is followed to avoid any obstacle that the vehicle may face in the X-Y plane during the horizontal forward vehicle navigation.

Now, the behaviour of the proposed OAWPF algorithm to avoid vertical obstacles will be evaluated using different vertical obstacle examples. The vehicle's travelling depth is kept constant, 3 meters as an example in the present model, to maintain following the planned path. Note that any travelling altitude can be selected. When detecting a vertical obstacle, the obstacle altitude is fed continuously to the system by the forward-looking sonar and the OAWPF algorithm is activated to avoid the obstacle. Figs. 11, 12, and 13 demonstrate three types of vertical obstacles: sloping, conical, and step up-down obstacles. The solid lines shown in Figs 11a, 12a, and 13a represent the dynamic paths calculated by the OAWPF algorithm. As seen from the figures, the vehicle path through the obstacle is steady and smooth, and safely considers the shape and dimensions of the obstacle.
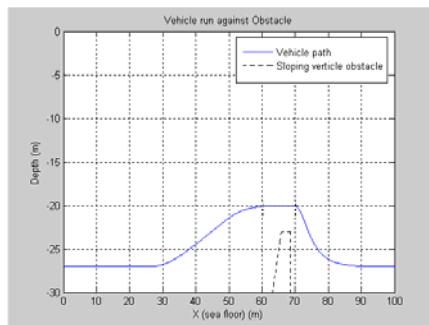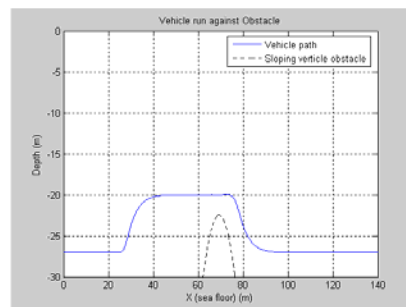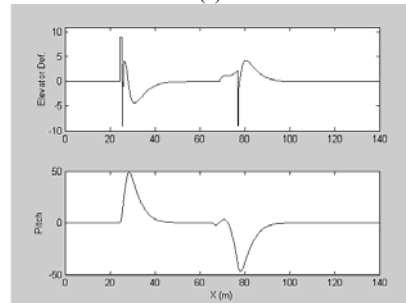

(a)
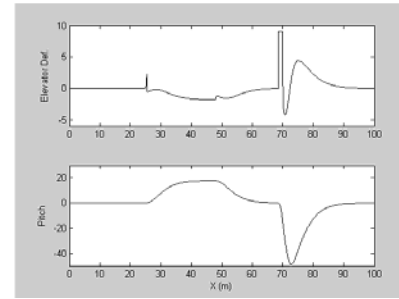
(b)

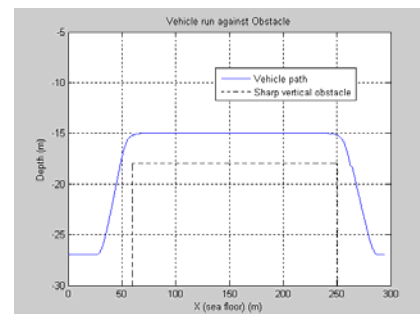Fig. 11 The vehicle dynamic path against obstacle (a), and the dynamic commands elevator and pitch deflections.

(a)

(b)

Fig. 12 The vehicle dynamic path against obstacle (a), and the dynamic commands elevator and pitch deflections.
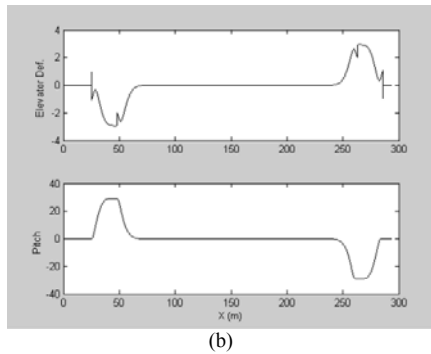

(a)

(b)

Fig. 13 The vehicle dynamic path against obstacle (a), and the dynamic commands elevator and pitch deflections.

The system output elevator deflection commands shown in Figs. 11b, 12b, and 13b are fast and smooth.

Thus, the vehicle overcomes the obstacle and then goes back to the planned path altitude. The resulting pitch angles are calculated and drawn in the prescribed figures. A vehicle path of 600 m and having three different vertical obstacles is shown in Fig. 14.
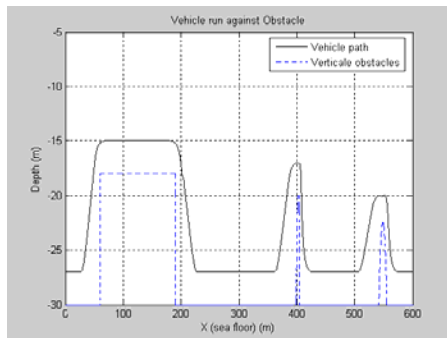

Fig. 14 Vehicle run against three different successive obstacles.

The figure introduces the vehicle obstacle avoidance while path following utilizing the OAWPF algorithm. The vehicle 3D trajectory is demonstrated in Fig. 15a.
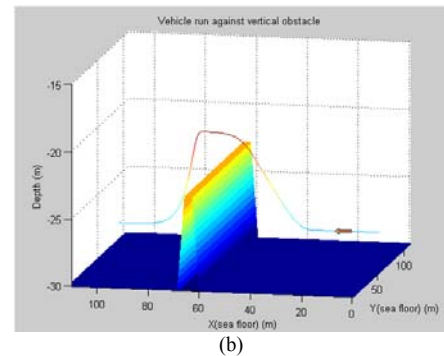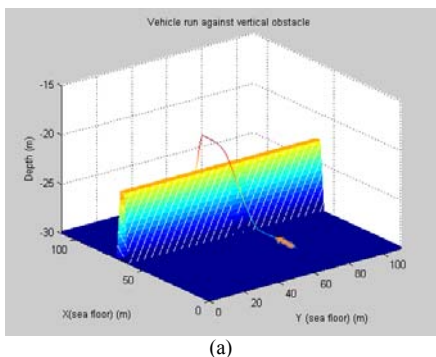

(a)

(b)

Fig. 15 3D plot of the vehicle run against a vertical obstacle while path following.

To see the hidden part of the trajectory that lies behind the obstacle, Fig. 15a is slightly rotated right to produce Fig. 15b. From the shown 3D figures, the vehicle trajectory is considered smooth, stable, and safe.

8. Conclusion

The simulation results and figures show that the proposed algorithm is robust and dynamic, and offers safe navigation in a sea floor having different types of obstacles. The algorithm behaviour is successfully tested in avoiding different obstacle shapes and dimensions while the vehicle follows its pre-designed mission path in both horizontal plane, assuming eight obstacles, and vertical plane, assuming three obstacles.

It is proved that the algorithm is dynamic and flexible. The algorithm can manipulate changes in initial planned path data, like waypoints, path tracks, or vehicle maintained depth. Changing the forward-looking sonar characteristics, like horizontal distance, is also accepted. Fig. 16 shows a new run assuming a 100 m horizontal sonar-detectable distance.
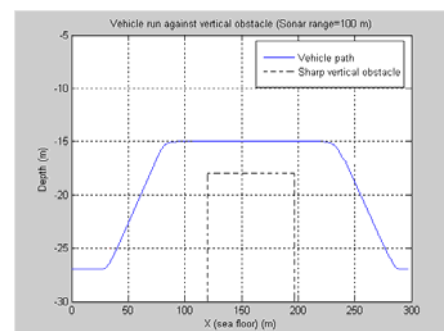

Fig. 16 A 100 m sonar-detectable horizontal distance.

References

[1] E. Bovio, D. Cecchi, F. Baralli, "Autonomous underwater vehicles for scientific and naval operations", Elsevier, Annual Reviews in Control 30 pp 117–130, 2006.

[2] J. YUH, "Design and Control of Autonomous Underwater Robots: A Survey", Autonomous Robots 8, 7–24, Kluwer Academic Publishers, The Netherlands, 2000.

[3] Autonomous Undrewater Vehicle REMUS: http://www.whoi.edu/science/PO/people/ashcherbina/capecod/remus.html

[4] Hydroid Inc., Homepage [www.hydroidinc.com], February 2009.

[5] Neal M. Patel, Shawn E. Ganoy, John E. Renaud z, Jay D. Martinx, Michael A. Yukish, " Simulation Model of an Autonomous Underwater Vehicle for Design Optimization", 45th AIAA/ASME/ ASCE/AHS/ASC Structures, Structural Dynamics & Materials Conference 19 - 22 April 2004, Palm Springs, California, USA.

[6] Fodrea, Lynn, Healey, A. J., "Obstacle Avoidance Control for the REMUS Autonomous Underwater Vehicle", Proceedings of the IFAC GCUUV Conference, Swansea, Wales, 2003.

[7] Healey, A. J., "Obstacle Avoidance While Bottom Following for the REMUS Autonomous Underwater Vehicle" Proceedings of the IFAC-IAV 2004 Conference, Lisbon, Portugal, July 5-7, 2004.

[8] C. Silvestre_, A. Pascoal, "Depth control of the INFANTE AUV using gain-scheduled reduced order output feedback", Elsevier Ltd., 2006.

[9] Heminger Dan L. ''Vertical Plane Obstacle Avoidance and Control of the REMUS Autonomous Underwater Vehicle using Forward Look Sonar'', Naval Postgraduate School, June 2005.

[10] Pramod Maurya, E. Desa, A. Pascoal, E. Barros, G. Navelkar, R Madhan, A. Mascarenhas, S. Prabhudesai, S.Afzulpurkar, A. Gouveia, S. Naroji, L. Sebastiao, " Control of the MAYA AUV in the Vertical and Horizontal Planes: Theory and Practical Results", Proceedings of the 7th IFAC Conference on Manoeuvring and Control of Marine Craft. Instituto Superior, Lisbon, Portugal, 2006.

[11] Timothy Prestero, " Verification of a Six-Degree of Freedom Simulation Model for the REMUS Autonomous Underwater Vehicle", MSc. Thesis, MIT, 2001.

[12] Geraint Paul Bevan, " Development of a Vehicle Dynamics Controller for Obstacle Avoidance", PhD. thesis, Glasgow, 2008.

[13] Christopher D. Chuhran, " Obstacle Avoidance Control for the REMUS Autonomous Underwater Vehicle", MSc. thesis, NPS, 2003.

[14] Healey A. J., and Lienard D. E. , " Multivariable Sliding Mode Control for Autonomous Diving and Steering of Unmanned Underwater Vehicles", IEEE Journal of Oceanic Engineering. Vol. 18, no. 3, pp. 327-339. July 1993.

Sami A. Mostafa
He received his BSc. In 1977 from Military Technical College,MSc. and PhD. From Ain Shams University Electronics and Communications 1983, and 1996 respectively. He holds the certificate of consultant engineer in Electrical projects management. He is now an Associate Professor, Electronics Department, Faculty of Industrial Education, Suez Canal University. His research and teaching interests focus on Radar Signal Processing, Wireless Communications, Air, surface, and Unmanned Vehicles path planning, and Mechanical to Electrical Power Conversion.

Ayman M. M. Brisha
B. Sc from Faculty of Engineering, Al_azhar University 1992, M. Sc., Computer Science & Control, From Eindhoven Technical University in cooperation with Fontys University, Netherlands 1998, Ph. D, Computer Science Engineering, Moscow Power. Engineering Institute (MPEI) (Technical University (TU)) Russia. IEEE active member, membership No. 1-1190593612, Active member in IAENG My member Number is: 102369– international journal for engineering research Member, Egyptian Engineering Syndicates (Computer Branch). He is now an Assist. Prof., Electronic depart, Faculty of Industrial Education, Beni-Suef University, Egypt.